

PROPELLER-ROTOR WHIRL FLUTTER:

A STATE-OF-THE-ART REVIEW

By Wilmer H. Reed III

NASA Langley Research Center  
Langley Station, Hampton, Va., U.S.A.

Presented at the Symposium on the Noise and Loading Actions on  
Helicopter V/STOL Aircraft and Ground Effect Machines

FACILITY FORM 602

**N66-22179**

(ACCESSION NUMBER)	<u>44</u>	(THRU)	<u>1</u>
(PAGES)	<u>TMX 56678</u>	(CODE)	<u>01</u>
(NASA CR OR TMX OR AD NUMBER)		(CATEGORY)	

Southampton, England  
Aug. 30-Sept. 3, 1965

GPO PRICE \$ \_\_\_\_\_

CFSTI PRICE(S) \$ \_\_\_\_\_

Hard copy (HC) 2.00

Microfiche (MF) ●

*TMX 56678*

PROPELLER-ROTOR WHIRL FLUTTER:

A STATE-OF-THE-ART REVIEW

By Wilmer H. Reed III\*

NASA Langley Research Center  
Langley Station, Hampton, Va., U.S.A.

- ABSTRACT

22/79

==

The basic phenomenon of propeller whirl instability in connection with conventional and V/STOL aircraft is described; theoretical and experimental investigations of the problem from the time it first became of concern on contemporary turboprop aircraft to the present are summarized; and some consideration is given to possible future configurations having hinged or highly flexible propeller-rotors.

Reed

==

INTRODUCTION

Although the phenomenon known as propeller whirl flutter - a dynamic instability that can occur in a flexibly mounted aircraft engine-propeller combination - was discovered analytically by Taylor and Browne in 1938 (ref. 1), it was not until its "rediscovery" in 1960 that it became a problem of practical concern.

Following the loss of two turboprop aircraft in fatal accidents it was established in wind-tunnel investigations (ref. 2) that propeller whirl flutter could have occurred if the nacelle stiffness was severely reduced, say by a structural failure. In the undamaged condition the aircraft had an adequate margin of safety from whirl flutter. In addition to this wind-tunnel

---

\*Assistant Head, Aeroelasticity Branch, Dynamic Loads Division.

~~CONFIDENTIAL~~  
~~NASA~~

investigation for a specific configuration some generalized trend studies were also conducted at NASA-Langley in order to identify and study the basic parameters involved in propeller whirl flutter (refs. 3 through 6).

As a result of these experiences on a turboprop aircraft, and the fact that VTOL configurations are likely to have unconventional propeller-rotor systems, whirl flutter has now become a design consideration on new propeller-driven aircraft. These considerations are reflected in recent amendments to U.S. Civil Air Regulations (ref. 7) which require that whirl flutter be included as a part of the dynamic evaluation of transport aircraft, and that no flutter shall occur as a result of failure of any single element of an engine mount structure.

The purpose of this paper is to review some progress that has been made in the area of propeller whirl flutter since the time the phenomenon became the subject of intensive study in 1960. Following a description of the basic mechanism of propeller whirl flutter, the paper summarizes some principal findings of generalized trend studies for idealized systems, and then illustrates how these results can be altered by the use of propeller-rotors with hinged blades and with highly flexible twisted blades. In addition, the paper reviews the status of propeller aerodynamic coefficients used for the prediction of whirl flutter on conventional and VTOL aircraft; discusses some effects of wing flexibility on whirl flutter; and, finally, cites an example wherein whirl flutter of a specific VTOL configuration is studied by means of an aeroelastically scaled wind-tunnel model.

## SYMBOLS

$$A_m = \int_{\epsilon}^1 \frac{\eta^{m-1}}{w} d\eta \quad m = 1, 2, \dots, 5$$

$$A_{\epsilon} = A_5 - 2\epsilon A_4 + \epsilon^2 A_3$$

a           nondimensional distance between nacelle pivot point and plane of propeller in propeller radii

$C_T$        thrust coefficient,  $\frac{\text{Thrust}}{\rho \left(\frac{\Omega}{2\pi}\right)^2 (2R)^4}$

c           propeller chord

$c_{l\alpha}$        lift-curve slope

$c_{\theta}, c_{\psi}$    nacelle viscous damping factors in pitch and yaw directions

e           hinge offset distance on flapping-blade propeller

$F + iG$    oscillating lift function

H           propeller-tip-speed ratio,  $\frac{\pi V}{\Omega R}$

I           total moment of inertia of system about pivot

$$I_1 = \frac{N}{2} \int_0^R m r^2 dr$$

$$I_2 = \frac{N}{2} \int_e^R m r(r - e) dr$$

$$I_3 = \frac{N}{2} \int_e^R m (r - e)^2 dr$$

$I_x$        mass moment of inertia of propeller about rotation axis,  $2I_1$

$$i = \sqrt{-1}$$

J           advance ratio,  $\frac{\pi V}{\Omega R}$

$$K = \frac{c_l \alpha^2 \rho c R^4 N}{4}$$

$M_\theta, M_\psi$  aerodynamic moments about nacelle pivot point

$m$  propeller blade mass per unit length

$N$  number of blades

$R$  propeller radius

$r$  local blade radius

$$S = \frac{N}{2} \int_e^R m(r - e) dr$$

$S_\theta, S_\psi$  rotational spring constants of nacelle

$V$  flight velocity

$$W = \sqrt{\left(\frac{V}{\Omega R}\right)^2 + \left(\frac{r}{R}\right)^2}$$

$e$   $\frac{e}{R}$ , hinge offset

$\zeta$  viscous-damping relative to critical damping of engine mount system

$\theta, \psi$  pitch and yaw angles of propeller shaft relative to static thrust axis

$\lambda = \mu + i\nu$  root of characteristic equation

$\mu$  damping ratio (+ unstable, - stable)

$\nu = \frac{\omega}{\Omega}$  whirl frequency ratio (+ for forward mode, - for backward mode)

$$\nu_0 = \frac{\omega_\theta}{\Omega}$$

$\rho$  air density

$\Omega$  propeller rotational frequency

$\omega$  propeller whirl frequency

$\omega_b$  cantilever fundamental frequency of nonrotating propeller blade

- $\omega_\theta, \omega_\psi$  uncoupled pitch and yaw frequencies of system with nonrotating propeller
- $\omega_h$  uncoupled wing bending frequency for rigid nacelle and nonrotating propeller
- $\omega_1$  fundamental wing coupled bending-torsion frequency for rigid nacelle and nonrotating propeller

### MECHANISM OF PROPELLER WHIRL FLUTTER

In order to introduce the basic ingredients of propeller whirl flutter it is convenient to reduce the problem to its most elementary form as was done in references 3 through 6. In figure 1 the sketch represents an idealized system in which the power plant or nacelle is assumed to be restrained by a set of springs and dampers at a pivot located behind the propeller disk. If the propeller blades and the nacelle structure are considered to be rigid, the dynamic behavior of the system can be described in terms of  $\theta$  and  $\psi$  which represent small angular deflections in pitch and yaw of the propeller axis relative to the static equilibrium position. The equations of motion, also shown in figure 1, indicate the nature of the various forces involved. Note that, in addition to the usual dynamic forces associated with inertia, damping, and elastic properties of the system, gyroscopic and aerodynamic forces are introduced by the rotating propeller.

The dynamic behavior of this system can be illustrated with the aid of the sketches in figure 2. The sketches on the left indicate that with a non-rotating propeller and with aerodynamic forces neglected, natural vibrations can occur independently in either the pitch plane or the yaw plane. There is no coupling between these two modes. However, with a rotating propeller

(center sketch) the original pitch and yaw modes no longer occur independently, but are coupled by gyroscopic action of the spinning propeller. The natural modes in this case are referred to as "whirl" (or precession) modes in reference to the manner in which the propeller hub whirls about the static thrust axis. As the rotational speed of the propeller increases, the frequency of one whirl mode increases while that of the other decreases. The higher frequency mode is known as the "forward whirl mode" because the direction of whirl is the same as that of the rotating propeller. Similarly, the lower frequency mode is known as the "backward whirl mode" because its rotational direction is opposite to that of the propeller.

It can be shown that if the propeller blades are rigid and there are no aerodynamic forces on the propeller this mechanical system is always stable. However, since whirl modes produce angle-of-attack changes on blade elements of the propeller, aerodynamic forces are generated, and it is these forces that provide the mechanism for an instability. Thus, just as in classical wing flutter, if the forward velocity of the system exceeds a certain critical value a dynamic instability can be encountered. This instability for rigid-blade systems invariably occurs in the backward whirl mode.

The sketches on the right-hand side of figure 2 give an example of the manner in which the system would respond in the backward whirl mode following a disturbance such as a gust. When the airstream velocity is less than the whirl flutter velocity,  $V_{crit}$ , the path traced by the propeller hub is a spiral that converges to the original static equilibrium position. When the flutter speed is exceeded, however, a small disturbance will result in a diverging spiral motion of the hub which will continue to build up until the structure fails or its motion becomes limited due to nonlinearities.

## PROPELLER-ROTOR SYSTEMS: RIGID AND NONRIGID BLADES

The generalized studies of classical propeller whirl flutter in references 3 through 6 were restricted to rigid propellers. This is a reasonable assumption for conventional propeller-driven aircraft; however, V/STOL designs often incorporate flexible and articulated propeller-rotors that are compromises between the long flexible blades of a helicopter rotor and the short stiff blades of an aircraft propeller. It is therefore of interest to consider the manner in which whirl flutter might be altered by the use of nonrigid propeller-rotors. Of equal interest here is also the question of how rotor mechanical instability - an instability fed by energy of the rotating rotor rather than by the airstream - might be altered by the inclusion of propeller-whirl-type aerodynamic forces.

For this purpose we will investigate some stability characteristics of the three systems shown schematically in figure 3. These systems each consist of a four-bladed propeller-rotor mounted, for convenience, on an axisymmetrical nacelle (in which stiffness and inertia properties are the same in the pitch and yaw directions). The first system to be considered here has rigid blades; the second system is like the first except the blades are hinged so as to allow flapping in the direction normal to the propeller disk plane; and the third is a system with a flexible twisted propeller-rotor. The vibration modes of importance for each of these systems are indicated by the sketches in figure 3.

### Résumé of Rigid-Blade Cases

The basic phenomenon of propeller whirl flutter for systems that comprise a rigid propeller and a flexibly mounted power plant, such as that illustrated in figure 1, is now reasonably well understood. The stability characteristics



of such systems have been investigated analytically over a rather broad range of parameters by Reed and Bland (ref. 3), Houbolt and Reed (ref. 4), and Sewall (ref. 5). In addition, wind-tunnel studies have been conducted by Bland and Bennett (ref. 6) to evaluate the theoretical prediction of propeller aerodynamic derivatives as well as whirl flutter stability boundaries.

A general finding of these studies is that whirl flutter is strongly dependent on three basic system parameters: the stiffness, the damping, and the pivot location. The influence of these parameters on whirl flutter is typically as shown in figure 4. For example, figure 4(a) illustrates the effect of the ratio of pitch stiffness to yaw stiffness on the stability of a system. Note in particular that the whirl flutter boundary is extended along the diagonal ray  $S_\theta = S_\psi$ ; this indicates that if a system had equal pitch and yaw stiffnesses it would be more prone to flutter than if one of the stiffnesses was appreciably reduced. The shape as well as the location of this curve, however, may be altered appreciably by the amount of structural damping in the system (see ref. 4). The lines that intersect each end of this boundary denote the stiffnesses required to prevent static divergence of the system.

Figure 4(b) is presented to illustrate the powerful stabilizing influence of mechanical damping on whirl flutter. It is interesting to note that if structural damping were assumed to be zero in whirl flutter analyses, as may be done frequently in wing flutter analyses, the stiffness required to prevent flutter would, in many cases, be grossly overestimated. As has been remarked by A. L. Head in a discussion of propeller whirl considerations on the XC-142, "a little damping goes a long way."

Finally, figure 4(c) shows that the further the pivot point is moved from the propeller disk the more stable the system becomes. This fact, incidentally,

can be attributed to the aerodynamic damping associated with transverse velocities of the propeller hub. The effects of the parameters indicated in figure 4 and other parameters, such as advance ratio, thrust, propeller rotational frequency, air density, etc., are investigated in detail in the previously mentioned generalized trend studies.

### Flapping Blades

The effects of flapping hinged blades on whirl flutter have been examined in several recent studies. The most comprehensive of these is the study by Richardson and Naylor (ref. 8) in which a considerable number of parametric variations were investigated analytically and some complementary test data presented for a low-speed wind-tunnel model. Wind-tunnel experiments of this type have also been conducted by E. F. Baird of Grumman Aircraft (unpublished) and by Reed and Bennett in reference 9. In addition, a whirl flutter analysis for a specific V/STOL configuration which utilizes flapping-blade propellers is presented by Gallardo and Flannelly in reference 10.

The results which follow are based on a whirl flutter analysis of the model tested by Reed and Bennett in reference 9. This model shown in figure 5 consisted of a windmilling propeller mounted on a spring restrained rod which could rotate in pitch and yaw about a set of gimbal axes behind the propeller. The blades are attached to the hub by means of pins in a manner such that they can be either fixed relative to the hub (the rigid-blade case) or allowed to flap about one of two possible hinge locations. The hinges are oriented so that the blades flap in the direction perpendicular to the plane of the propeller disk.

The theoretical analysis used is based on equations developed in reference 8 wherein the dynamics of the system are expressed in terms of four degrees of freedoms: pitch and yaw of the propeller disk about the gimbal axis and cyclic flapping of the blades in the pitch and yaw directions normal to the propeller plane. For an axisymmetric system, such as the one treated herein, the number of degrees of freedom conveniently can be reduced from four to two. This simplification is made possible by the use of two complex coordinates to represent the circular whirl modes of the system in place of four real coordinates to represent separately the pitch and yaw modes involved. For the sake of completeness, the final form of the flapping-blade system characteristic equation, based on derivations in reference 8, is presented in the appendix of this paper. The physical parameters of the model tested in reference 9 are given in table I.

Theoretical results for the model with rigid blades are presented in figure 6. This figure shows in a nondimensional form the variation of natural frequency and damping of the system (obtained from the roots  $\lambda = \mu + i\nu$  of the characteristic equation in the appendix) as a function of the frequency ratio  $\Omega/\omega_0$ , where  $\Omega$  is the propeller frequency and  $\omega_0$  the nacelle pitch or yaw frequency with a nonrotating propeller. Since the propeller is windmilling,  $\Omega$  is proportional to the airstream velocity. In the plots of frequency ratio, obtained from the imaginary part of a root, positive values denote forward whirl modes and negative values, backward whirl modes; in the plots of damping ratio, obtained from the real parts of the roots, a negative value indicates a stable system and a positive value, an unstable system. These results illustrate some characteristic features of propeller whirl flutter: the instability develops in the backward whirl mode and there is no

evidence of coupling between the two whirl modes involved. Because of this latter feature, it has been observed in reference 8 that propeller whirl may be regarded as a type of single-degree-of-freedom flutter so long as the mode considered is a whirl mode. For the system shown in figure 6 whirl flutter is predicted when the parameter  $\frac{\Omega}{\omega_0} \geq 2.9$ . The corresponding whirl flutter frequency is seen to be about  $0.5\omega_0$ .

Consider next the dynamic characteristics of the system when the blades are free to flap normal to the propeller rotation plane. A plot of the type shown in figure 6 for rigid blades is shown in figure 7 for the same model hinged blades. The hinge offset is  $0.13R$  from the propeller rotation axis. Motion of the system is now characterized by four vibration modes. In all but one of these modes the stability increases continuously with increasing speed. The mode in which the instability develops is, as in the case of rigid blades, a backward whirl mode; however, the flutter velocity is about two and one-half times higher than it was for fixed blades ( $\Omega/\omega_0 = 7.5$  as compared with 2.9). Also shown in figure 7 are the natural vibration mode shapes of the system at the flutter speed. Note that there is relatively little blade flapping present in the flutter mode which is identified as (2) in the figure. (These modes were calculated for the propeller speed corresponding to flutter but with aerodynamic and damping forces ignored.)

Figure 8 shows a comparison between theory and experiment for the model tested in reference 9. For the rigid-blade case and for the 13-percent hinge offset case flutter occurred in the backward whirl mode both in the theory, as indicated in figures 6 and 7, and in the tests. However, in the experiment the model with the 8-percent hinge offset fluttered in the forward whirl mode at a much lower velocity than did either of the other configurations. This forward

whirl flutter was not predicted by the analysis, however nonlinearities may have been involved since the motion was amplitude limited and could only be initiated when the disturbing force exceeded a certain threshold level. It should be noted that Richardson's model with flapping blades also encountered forward whirl instabilities (ref. 8). The only way that the analysis could be made to predict such an instability was to introduce large phase lags between the displacements of the propeller axis and the associated aerodynamic forces on the blades. (These aerodynamic lag effects are related to the unsteady helical wake behind the propeller.) For example, the assumption of a  $30^\circ$  phase lag resulted in forward-whirl flutter for the configuration tested in reference 8. For the configuration considered in this paper, however, aerodynamic phase lags as high as  $45^\circ$  were assumed but an instability in the forward whirl mode could never be predicted. (The phase lag assumed in the calculations for fig. 6 was  $15^\circ$ .)

#### Flexible-Twisted Blades

Bending deformations of a twisted propeller blade differ from those of the previously discussed flapping blade in a fundamental way. Whereas the flapping motion of a hinged blade was assumed to be normal to the propeller plane, the bending motion of a flexible blade with twist has components of displacement in the propeller plane as well as components normal to the plane. The relative contribution of these two components to a bending vibration mode of a blade will depend on such factors as its geometric pitch angle and the spanwise location of the root chord (i.e., the hub diameter).

These in-plane motions permitted by blade flexibility make possible the occurrence of another class of self-excited vibrations which, unlike propeller whirl flutter, is purely mechanical in origin. This phenomenon, popularly

called "ground resonance," has received considerable attention in helicopter studies (e.g., refs. 11 and 12) and has also been recognized as a potential problem on tilt-wing V/STOL configurations (ref. 13).

A recent study of the interaction between propeller whirl flutter and mechanical instabilities on systems having flexible-twisted propellers has been conducted by Richardson, McKillop, et al. (ref. 14). In this study, as in reference 8 for hinged propellers, a considerable number of parametric variations were analyzed theoretically and wind-tunnel tests were conducted on a simple low-speed wind-tunnel model.

The mathematical and physical models considered by Richardson consisted of an axisymmetrical nacelle, and a flexible twisted propeller having a rigid hub and three or more uniform constant-chord blades. The relevant blade bending modes which can couple with whirl flutter are shown to be cyclic "pitch" and cyclic "yaw" type motions in which the tip path plane is pitched or yawed due to blade bending. Each of these modes has associated with it an in-plane component of displacement. The flexible-blade mode illustrated in figure 3, for example, is the "pitch" mode accompanied by in-plane bending. It is remarked that coning motions of the blades do not couple with the modes involved in the whirl instabilities and consequently this mode was not included in the analysis.

Some principal findings of the studies in reference 14 are presented in figures 9 and 10 of this paper. Figure 9 shows the stability characteristics of one of the configurations analyzed for a condition of zero damping and without aerodynamic forces (e.g., as in a vacuum). There is close similarity between these plots and frequency diagrams for mechanical instability obtained by Coleman (ref. 11). As the propeller rotational speed  $\Omega$  increases a point

is reached where two of the frequencies coalesce, resulting in two modes at the same frequency, one of which is damped and the other unstable. This point, denoted by A in the figure, marks the beginning of a region of mechanical instability in a forward whirl mode.

Figure 10 shows the effects of adding aerodynamic forces to the stability analyses by progressively increasing air density from zero, the value assumed in figure 9. (Point A in fig. 9 lies on the zero density curve in fig. 10.) Stability boundaries are presented in figure 10 as plots of blade frequency against nacelle frequency for both forward and backward whirl modes. Boundaries for the forward mode originate from a mechanical instability, and those for the backward mode originate from a whirl flutter instability.

Note that in the forward whirl mode as air density increases two regions of instability develop. The region that has the higher values of  $\omega_{\theta}/\Omega$  is not of practical significance because the rate of growth of the unstable motions involved was found to be extremely low and would be eliminated by a small amount of structural damping. The other region of instability in the forward whirl mode is initially made worse as density increases, but with further increase in density the area of instability is reduced and eventually eliminated. It is interesting to note from this figure that the system encounters mechanical instabilities only if the nonrotating blade natural frequency,  $\omega_b$ , is less than the rotational frequency of the propeller.

With regard to propeller whirl flutter - indicated by the stability boundaries for the backward mode - it appears that blade flexibility has relatively little effect except in a region where the blade frequency parameter is near unity. The asymptotic boundaries for a rigid propeller are also shown for comparison.

## PROPELLER AERODYNAMICS

As has already been mentioned in a previous section of the paper the pitching and yawing oscillations that accompany propeller-nacelle whirl motions produce aerodynamic forces on the propeller which in turn provide the driving mechanism for instability. Several methods are available for predicting the aerodynamic forces and moments required in a whirl flutter analysis. Ribner's analysis of yawed propellers (ref. 15) has long been used in studies of aircraft stability and is equally useful in propeller whirl flutter studies (see, for example, ref. 3). Houbolt's strip theory analysis in reference 4 lacks some of the refinements of Ribner's method, but is simpler to apply and appears to give comparable results. Both of these theories are based on the assumption that the inflow angle is small and the aerodynamic forces are "quasi-static," i.e., oscillating wake effects are ignored.

### Measured Derivatives

To evaluate theoretical methods for predicting propeller whirl flutter, Bland and Bennett (ref. 6) have conducted an experimental investigation on a model which resembles the simple mathematical models previously studied. The wind-tunnel model consisted of a windmilling propeller mounted on an isolated nacelle which had symmetrical stiffness in pitch and yaw. Measurements of static aerodynamic propeller derivatives and whirl flutter boundaries for the same propeller system were obtained over a range of test conditions. Typical results from the study are presented in figure 11 which shows the nacelle damping required to prevent flutter plotted against a nondimensional velocity. The calculated flutter boundaries were determined on the basis of three sets of aerodynamic derivatives: the theoretical derivatives derived by the methods



of references 4 and 15, and the actual derivatives as measured on the model. Note that the calculations based on measured derivatives are in excellent agreement with the experimental data, whereas those based on theoretical derivatives follow the same trends but tend to underestimate the observed flutter speed.

#### Unsteady Flow

These differences in the flutter boundaries based on theoretical and measured derivatives may in part be due to unsteady aerodynamic effects. It has been shown (e.g., ref. 3) that aerodynamic phase lags associated with the oscillatory wake have a stabilizing effect on the usual backward-mode whirl flutter. The theoretical derivatives used in figure 11 were modified to account for phase lags on the basis of the Theodorsen circulation function  $F + iG$  for two-dimensional airfoils. This is a good approximation for very large advance ratios; however, for smaller advance ratios, the circulation function is significantly altered due to the helical pattern of the wake.

In reference 16 Loewy derives modified  $F + iG$  function for a propeller with a helical wake. These results indicate that for low advance ratios the phase lag for a propeller can be much larger than would be predicted by the classical  $F + iG$  function for two-dimensional airfoils. It is interesting to note that for lowest advance ratios investigated by Bland and Bennett in reference 6 ( $J = 1.3$ ) the measured phase lag was  $24^\circ$  as compared with a theoretical value of  $13^\circ$  based on Theodorsen's function.

#### Thrust

It has been established theoretically that propeller thrust has a relatively insignificant effect on whirl flutter stability for conventional rigid propellers under high-speed flight conditions. This fact greatly simplifies

the construction and testing of wind-tunnel models in that it permits the use of windmilling rather than thrusting propellers. In a theoretical investigation of the effects of propeller thrust on whirl flutter, Ravera (ref. 17) shows that thrust causes large deviation in the propeller derivatives at low-speed high-thrust flight states, such as take-off. However, at higher forward speeds where whirl flutter normally occurs, the deviation between aerodynamic coefficients for thrusting and windmilling propellers is usually less than 5 percent. Similar conclusions are found in reference 9 on the basis of experimental coefficients obtained on a thrusting propeller.

It is pointed out in reference 17 that before drawing general conclusions regarding the effects of thrust on whirl flutter, one should examine the thrust characteristic curve of the propeller in question. If it is found, for example, that at high forward speeds the thrust is small relative to maximum thrust, the effects of thrust on the propeller coefficients may be ignored. This case, which is typical of most propellers, is illustrated in figure 12(a). On the other hand, if the propeller delivers a significant percentage of maximum thrust at high forward speeds, such as is illustrated in figure 12(b), thrust may well have an important influence on whirl flutter.

#### High Inflow Angles

In the transition maneuver of VTOL aircraft from vertical to horizontal flight the inflow angle - i.e., the angle between the thrust axis and the airstream - may be as large as  $90^\circ$ . At these high inflow angles the propeller aerodynamic derivatives are likely to have values that differ markedly from those corresponding to high-speed flight conditions (see refs. 18 and 19). Since whirl flutter is usually considered to be a relatively high-speed flight

phenomenon it is of interest to explore the possibility of encountering whirl flutter in low-speed flight during transition. This question was briefly examined in reference 9. On the basis of whirl flutter calculations which utilized experimental propeller derivatives and a simple axisymmetric nacelle, angle-of-attack effects were found to be stabilizing in that the stiffness required to prevent flutter at high inflow angles was slightly less than that required at low angles. These results are summarized in figure 13 for a windmilling and a thrusting propeller.

#### WING FLEXIBILITY

The propeller-nacelle systems considered in previous sections of the paper were assumed to have been flexibly mounted to a rigid wing or backup structure. This simplifying assumption is very useful, especially in preliminary design studies, in that it permits one to readily isolate the effects of various basic parameters. However, dynamic coupling between the propeller-nacelle system and the wing on which it is mounted can alter the whirl flutter boundaries predicted for a rigid wing. In general it has been found that wing aeroelastic effects have a stabilizing influence on whirl flutter.

This general trend and an exception to it can best be illustrated with the aid of figure 14. Stiffness boundaries of this type show the combination of pitch and yaw nacelle stiffnesses that would be required to avoid whirl flutter of a system for a given set of flight conditions. When the nacelle stiffnesses are greater than the minimum values indicated by these boundaries, propeller whirl flutter would not be encountered by the system. The curves presented in figure 14 are based on results obtained by Zwaan and Bergh in an analog computer study of whirl flutter (ref. 20). These curves show the influence of

wing flexibility on whirl flutter for three cases: (a) a rigid wing, (b) a wing having freedom to translate vertically, and (c) a wing having freedom to translate and rotate about an elastic axis. In the latter two cases, aerodynamic forces are assumed to act on the wing as well as on the propeller.

Consider first the case of a rigid wing. Features of this stability boundary are typical of those found in reference 4 and discussed here in figure 4(a). Again, it is to be noted that the boundary is extended along the diagonal ray  $S_\theta = S_\psi$  such that the symmetrical system, indicated by point A, is the most critical from the standpoint of whirl flutter. The points at which this curve, as well as other curves in the figure, terminate are the static divergence boundaries for the system.

When the wing has freedom to oscillate in vertical translation it can be seen that its effect on whirl flutter is always stabilizing. This increased stability can be attributed to aerodynamic damping forces on the wing. It is of particular interest to note the "necked down" portion of the curve where the stabilizing influence of the wing is most pronounced. At the points labeled B, the whirl frequency  $\omega$  coincides with the wing bending frequency  $\omega_h$  so that whirl motions of the propeller-nacelle tend to drive the wing at a resonant amplitude. Thus, Zwaan and Bergh suggest that the wing in this case may be considered as a type of tuned damper which absorbs greatest energy when the system frequency is close to the tuned frequency of the damper.

In the third case shown in figure 14 the wing vibration mode involves coupled bending and torsion motions. The frequency of the first coupled wing mode  $\omega_1$  in this case is approximately the same as the uncoupled bending frequency  $\omega_h$  discussed previously, but the mode shape indicates strong coupling between the bending and twisting motions  $h$  and  $\alpha$ . The stability boundary

for this condition illustrates an exception to the generally observed trend that wing flexibility stabilizes whirl flutter. It should be noted that the maximum stiffness  $S_0$  required occurs in the vicinity of point C where the wing fundamental coupled frequency  $\omega_1$  and the nacelle yaw frequency  $\omega_y$  are the same. Since the wing mode involves pitching of the propeller, point C may be regarded as a coincidence of "pitch" and yaw frequencies for the flexible wing just as point A was for the rigid wing. In both cases the region of instability is extended at these points where the pitch and yaw frequencies coincide.

Thus, a general conclusion reached in reference 20 is that a flexible wing has a stabilizing effect on propeller whirl flutter except possibly in a region where the uncoupled yaw frequency is close to a wing torsion frequency. Beneficial effects of a wing on whirl flutter have also been reported in references 21 and 22.

#### AEROELASTIC MODELS

Simplified mathematical and physical models, such as those discussed in this paper, provide valuable aids for gaining insight into a complex phenomenon and are useful in guiding the course of preliminary design. However, as the final design of an aircraft evolves, it is customary to employ more refined analytical and experimental techniques to insure that the flutter margin is adequate for any flight condition within the flight envelope. The analytical techniques used may involve separate consideration of whirl flutter and wing flutter, or the propeller-nacelle system may be included as additional ingredients in an aeroelastic stability analyses of the complete system. Similarly,

model testing techniques may vary in complexity from an isolated propeller-nacelle to an aeroelastically scaled model of the complete aircraft.

A specific example wherein propeller whirl flutter was a design consideration from the outset is provided by the XC-142A - a VTOL aircraft. A review of the wind-tunnel investigation of aeroelastic stability for the XC-142A is reported by Head and Smith in reference 22. This investigation involved an aeroelastic model in which each of four engine-gearbox-propeller systems was dynamically scaled. The propellers were nonpowered but were shafted together to insure that all turned at the same speed. The remarkable degree of detail achieved in the dynamic simulation of the engine-gearbox system is apparent in figure 15. The gearbox is connected to the engine by a multiredundant strut arrangement on the model in the same manner as it is on the aircraft. The flexibility of each strut as well as the overall flexibility between the engine and the gear box are accurately scaled in the model. The authors of reference 22 stated that the simulation of this component represented the most difficult design problem on the model.

A flutter design requirement for this aircraft is that no flutter shall occur as a result of failure of any single structural element (e.g., see ref. 7). Therefore, in the model tests a failure of various strut members was simulated by simply removing the strut in question. The strut failure conditions that were actually simulated on the dynamic model were selected on the basis of analysis. It is interesting to note that in some cases the calculated whirl flutter speed was increased as a result of a strut failure.

## CONCLUDING REMARKS

This paper has attempted to review the state-of-the-art of propeller whirl flutter and some recent contributions to it. On the basis of this review the following observations can be made:

1. Classical propeller whirl flutter in the backward whirl mode is amenable to analysis providing the propeller aerodynamic coefficients and the damping of the engine mount are known with reasonable accuracy. In most instances strip-theory methods appear adequate for determining the propeller aerodynamic coefficients.

2. The use of nonrigid propeller-rotors can have a significant influence on the whirl stability of a system. For instance, flapping blades introduce the possibility of flutter in the forward mode and flexible blades give rise to mechanical instabilities, however it was found that the propeller aerodynamic forces which create whirl flutter tend to mitigate mechanical instabilities.

3. The effects of high inflow angles and large thrust coefficients associated with VTOL transition maneuvers are relatively unimportant from the standpoint of whirl flutter.

4. Wing flexibility generally has a stabilizing effect on whirl flutter except when the nacelle uncoupled yaw frequency is close to the wing torsion frequency.

Finally, it should be remarked that the particular parameters selected for discussion in this paper, although representative, are not necessarily the only ones of significance with regard to whirl flutter. On specific configurations such factors as the interaction of whirl modes with thrust-control system dynamics, the operation of propeller-rotors as "pushers" which would have upstream pivot locations, or the coupling between whirl modes and in-plane

wing bending modes are likely to be important. If these factors are not important the dynamicist concerned with propeller-rotor systems should have no difficulty in discovering some others that are.



## APPENDIX

### STABILITY DETERMINANT FOR WHIRL FLUTTER OF PROPELLERS WITH HINGED BLADES

The equations used to calculate stability of the hinged-blade propeller model in figures 7 and 8 are based on derivations by Richardson and Naylor in reference 8. The equations of motion for the system are expressed in terms of four degrees of freedom: pitch and yaw of the propeller hub about a point aft of the hub, and cyclic (antisymmetric) flapping of the blades in the pitch and yaw directions. When the system has axial symmetry, as does the model under consideration, the whirl modes are circular (i.e., pitch and yaw motions are 90° out of phase and are of equal amplitude). For such conditions the equations of motion can be reduced from a set of four equations with real coefficients to a set of two equations with complex coefficients.

The stability determinant of the system in the notation of reference 8 is:

$$\left| \lambda^2 A + \lambda(B + D) + (C + E + \nu_N \hat{A}) \right| = 0$$

where  $\lambda = \mu + i\nu$  is a solution (eigenvalue) of the equation. The sign of  $\mu$  determines whether the system is stable (-) or unstable (+), and the sign of  $\nu$  (the nondimensional whirl frequency  $\nu = \omega/\Omega$ ) determines the direction of whirl. A positive sign represents forward whirl and a negative sign, backward whirl. The coefficients A, B, C, etc., are matrices that contain the inertia, gyroscopic, and aerodynamic parameters of the system. For the axisymmetric system under consideration these matrices are defined as follows:

$$[A] = \begin{bmatrix} I & I_2 \\ I_2 & I_3 \end{bmatrix}$$

$$[D] = \begin{bmatrix} (2\zeta v_0 I_y - i2I_1) & -i2I_2 \\ -i2I_2 & -i2I_3 \end{bmatrix}$$

$$[E] = \begin{bmatrix} 0 & 0 \\ 0 & eS \end{bmatrix}$$

$$[v_N \hat{A}] = \begin{bmatrix} v_0^2 I & 0 \\ 0 & 0 \end{bmatrix}$$

$$[B] = K \left[ \begin{array}{c|c} \begin{matrix} F(a^2 H^2 A_1 + A_5) \\ -iG(a^2 H^2 A_1 + A_5) \end{matrix} & \begin{matrix} F(A_5 - \epsilon A_4) + GaH(A_3 - \epsilon A_2) \\ + i[FaH(A_3 - \epsilon A_2) - G(A_5 - \epsilon A_4)] \end{matrix} \\ \hline \begin{matrix} F(A_5 - \epsilon A_4) - GaH(A_3 - \epsilon A_2) \\ -i[FaH(A_3 - \epsilon A_2) + G(A_5 - \epsilon A_4)] \end{matrix} & \begin{matrix} A_\epsilon(F - iG) \end{matrix} \end{array} \right]$$

$$[C] = K \left[ \begin{array}{c|c} \begin{matrix} -FaH^3 A_1 + GH^2 A_3 \\ + i(FH^2 A_3 + GaH^3 A_1) \end{matrix} & \begin{matrix} FaH(A_3 - \epsilon A_2) - G(A_5 - \epsilon A_4) \\ -i[F(A_5 - \epsilon A_4) - GaH(A_3 - \epsilon A_2)] \end{matrix} \\ \hline \begin{matrix} GH^2(A_3 - \epsilon A_2) \\ + iFH^2(A_3 - \epsilon A_2) \end{matrix} & \begin{matrix} -A_\epsilon(F + iG) \end{matrix} \end{array} \right]$$

The above matrices are of the form of those presented in reference 8; however additional terms, not explicitly given in reference 8, have been included here to represent unsteady aerodynamic effects ( $F + iG$ ) and viscous-type

structural damping  $\zeta$ . The parameters that make up the matrix elements are defined in the list of symbols and the numerical values of parameters used in the present calculations are given in table I.

## REFERENCES

1. Taylor, E. S., and Browne, K. A.: Vibration Isolation of Aircraft Power Plants. Jour. Aero. Sci., vol. 6, no. 2, Dec. 1938, pp. 43-49.
2. Abbott, Frank T., Jr., Kelly, H. Neale, and Hampton, Kenneth D.: Investigation of Propeller-Power-Plant Autoprecession Boundaries for a Dynamic-Aeroelastic Model of a Four-Engine Turboprop Transport Airplane. NASA TN D-1806, 1963.
3. Reed, Wilmer H., III, and Bland, Samuel R.: An Analytical Treatment of Aircraft Propeller Precession Instability. NASA TN D-659, 1961.
4. Houbolt, John C., and Reed, Wilmer H., III: Propeller-Nacelle Whirl Flutter. Jour. Aerospace Sci., vol. 29, no. 3, Mar. 1962, pp. 333-346.
5. Sewall, John L.: An Analytical Trend Study of Propeller Whirl Instability. NASA TN D-996, 1962.
6. Bland, Samuel R., and Bennett, Robert M.: Wind-Tunnel Measurement of Propeller Whirl-Flutter Speeds and Static-Stability Derivatives and Comparison With Theory. NASA TN D-1807, 1963.
7. U.S. Civil Air Regulations 4b.308 Amendment 4b-16, effective October 5, 1964.
8. Richardson, J. R., and Naylor, H. F. W.: Whirl Flutter of Propellers With Hinged Blades. Report No. 24, Engineering Research Associates, Toronto, Canada, March 1962.
9. Reed, Wilmer H., III, and Bennett, Robert M.: Propeller Whirl Flutter Considerations for V/STOL Aircraft. Cal/Trecom Symposium Proceedings, vol. III - Dynamic Load Problems Associated With Helicopters and V/STOL Aircraft, June 1963.

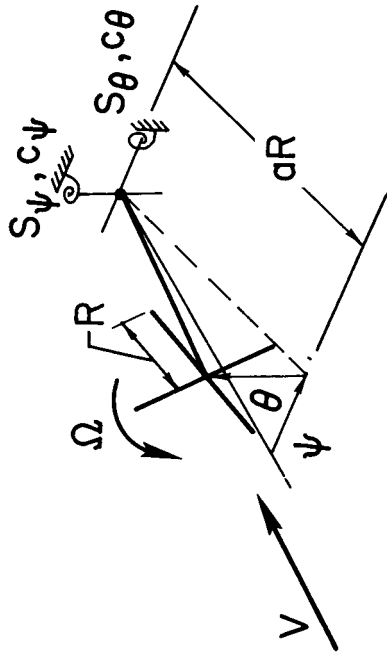
10. Gallardo, V. C., and Flannelly, William: Propeller-Nacelle Whirl Flutter Analysis of K-16B Amphibious VTOL/STOL Aircraft. Rept. No. G-113-41, Kaman Aircraft Corp., Aug. 1962.
11. Coleman, Robert P., and Feingold, Arnold M.: Theory of Self-Excited Mechanical Oscillations of Helicopter Rotors With Hinged Blades. NACA TR 1351, 1958.
12. Brooks, George W.: The Mechanical Instability and Forced Response of Rotors on Multiple-Degree-of-Freedom Supports. PhD Thesis, Princeton University, October 1961.
13. Loewy, Robert G., and Yntema, Robert T.: Some Aeroelastic Problems of Tilt-Wing VTOL Aircraft. Journal of the American Helicopter Society, vol. 3, no. 1, Jan. 1958.
14. Richardson, J. R., McKillop, J. A., Naylor, H. F. W., and Blandler, P. A.: Whirl Flutter of Propellers With Flexible Twisted Blades. Rept. No. 43, Engineering Research Associates, Toronto, Canada, Dec. 1963.
15. Ribner, Herbert S.: Propellers in Yaw. NACA Rep. 820, 1945. (Supersedes NACA ARR 3L09.)
16. Loewy, Robert G.: A Two-Dimensional Approximation to the Unsteady Aerodynamics of Rotary Wings. Jour. Aeronautical Sci., vol. 24, no. 2, Feb. 1957, pp. 81-92.
17. Ravera, Robert J.: Effects of Steady State Blade Angle of Attack on Propeller Whirl Flutter. Rep. No. ADR 06-01-63.1, Grumman Aircraft Eng. Corp., July 1963.
18. De Young, J.: Propeller at High Incidence. AIAA Jour. of Aircraft, vol. 2, no. 3, May-June 1965, pp. 241-249.

19. Shenhman, Albert M.: Generalized Performance of Conventional Propellers for VTOL-STOL Aircraft. Hamilton Standard Rept. No. HS-1829, March 1958.
20. Zwaan, R. J., and Bergh, H.: Restricted Report, F.228, Nat. Aero-Astronautical Research Inst., N.L.R., Amsterdam, Feb. 1962.
21. Bennett, Robert M., and Bland, Samuel R.: Experimental and Analytical Investigation of Propeller Whirl Flutter of a Power Plant on a Flexible Wing. NASA TN D-2399, 1964.
22. Head, A. L., and Smith, W. D.: Dynamic Model Testing of the XC-142A Aircraft. Proceeding of Symposium on Aeroelastic and Dynamic Modeling Technology, RTD-TDR-63-4197, Part I, March 1964.

TABLE I.- SYSTEM PARAMETERS USED IN CALCULATIONS  
 OF FLAPPING-BLADE MODEL FLUTTER BOUNDARIES  
 (SEE FIGS. 5 AND 8)

a . . . . .	0.25
c, (at 3/4R), ft . . . . .	0.0835
$c_{l\alpha}$ , per rad. . . . .	$2\pi$
eS, slug-ft <sup>2</sup> . . . . .	$0.0495 \times 10^{-4}$
*F + iG . . . . .	0.67 - i 0.18
J . . . . .	1.10
I, slug-ft <sup>2</sup> . . . . .	$1.310 \times 10^{-4}$
I <sub>1</sub> , slug-ft <sup>2</sup> . . . . .	$0.3816 \times 10^{-4}$
I <sub>2</sub> , slug-ft <sup>2</sup> . . . . .	$0.2586 \times 10^{-4}$
I <sub>3</sub> , slug-ft <sup>2</sup> . . . . .	$0.2090 \times 10^{-4}$
N . . . . .	4
R, ft . . . . .	0.50
$\epsilon$ . . . . .	0.137
$\zeta$ . . . . .	0.04
v <sub>0</sub> . . . . .	Varied

\*The F + iG functions employed here combine aspect ratio and phase lag corrections. The phase lag is based on experimental data.



EQUATIONS OF MOTION

PITCH:  $I\ddot{\theta} + c_{\theta}\dot{\theta} + S_{\theta}\theta - I_x\Omega\dot{\psi} = M_{\theta}$

YAW:  $I\ddot{\psi} + c_{\psi}\dot{\psi} + S_{\psi}\psi + I_x\Omega\dot{\theta} = M_{\psi}$

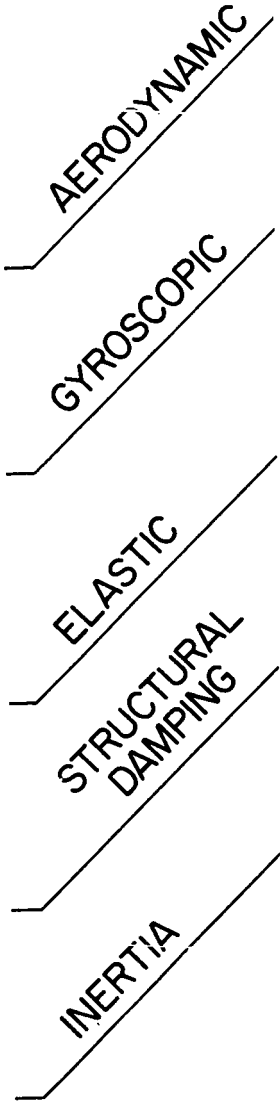


Figure 1.- Idealized propeller-nacelle systems.





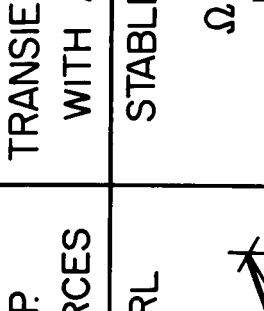
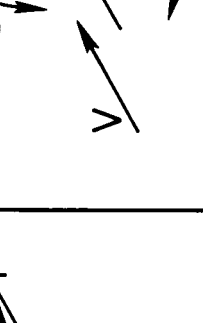

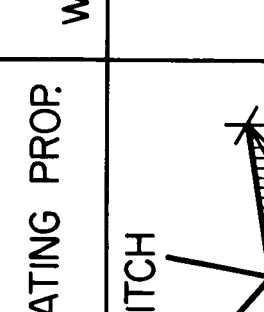
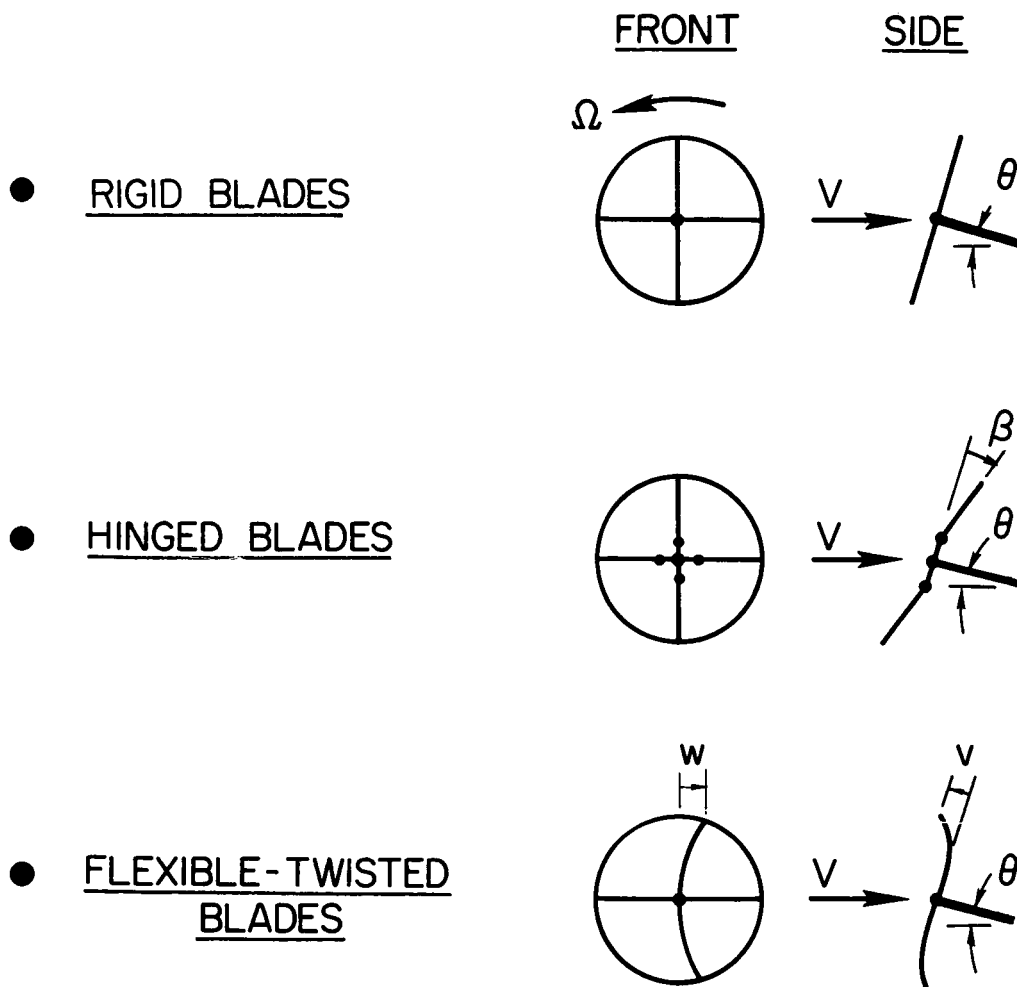
NONROTATING PROP.	ROTATING PROP. WITHOUT AIR FORCES	TRANSIENT RESPONSE WITH AIR FORCES
<p>PITCH</p> 	<p>FORWARD WHIRL</p> 	<p>STABLE (<math>V &lt; V_{CRIT.}</math>)</p> 
<p>YAW</p> 	<p>BACKWARD WHIRL</p> 	<p>UNSTABLE (<math>V &gt; V_{CRIT.}</math>)</p> 

Figure 2.- Natural vibration modes of system with rigid propeller.



NASA

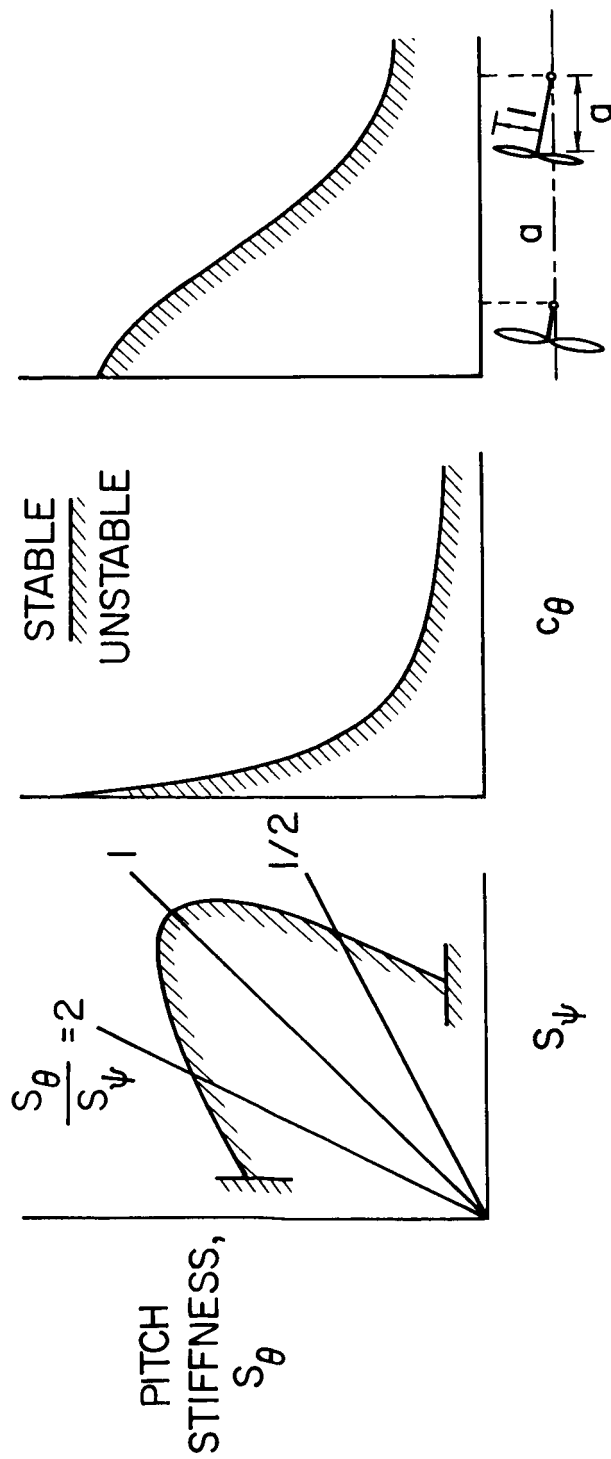
Figure 3.- Propeller-rotor systems considered.

(a) STIFFNESS RATIO

(b) NACELLE DAMPING

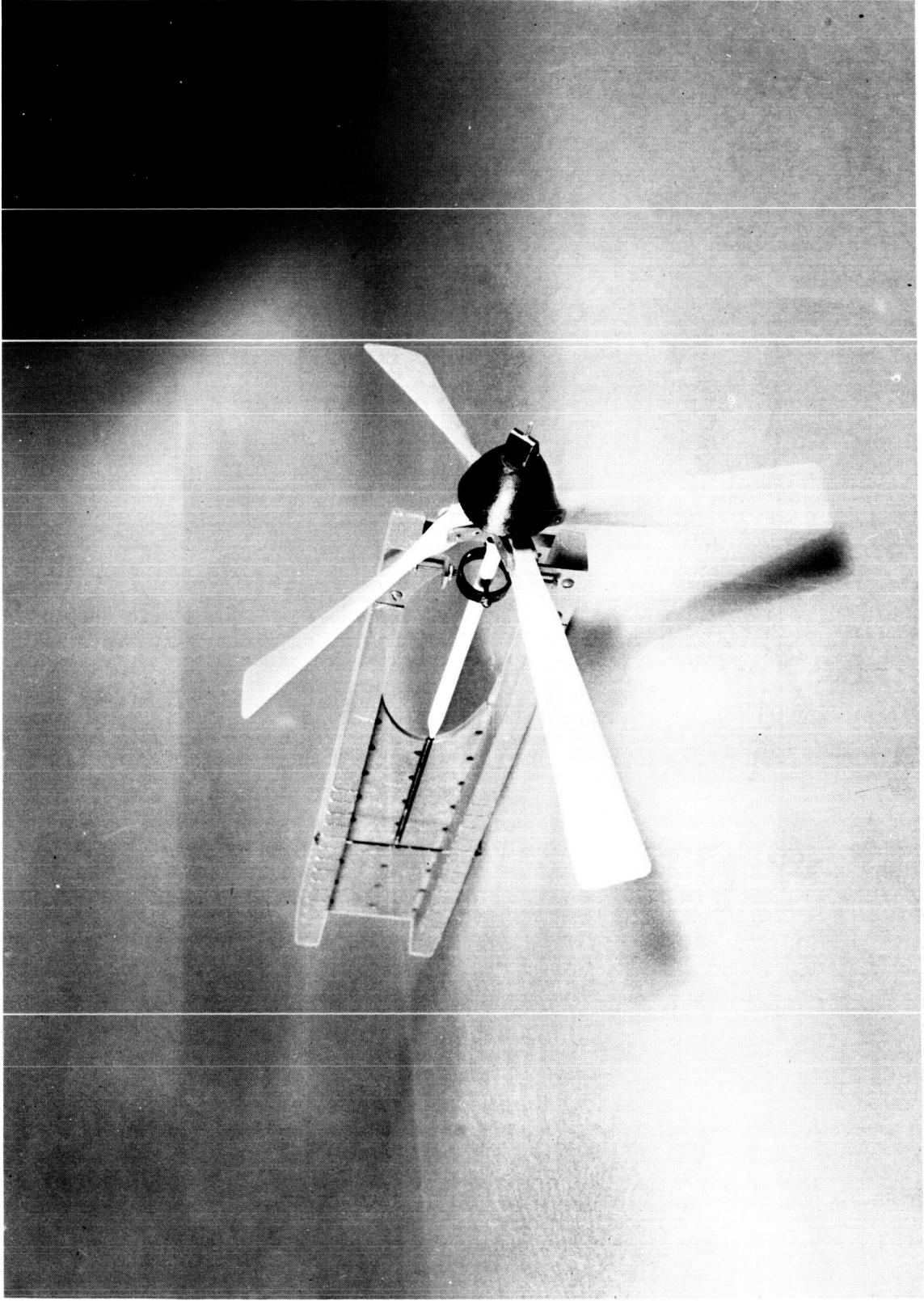
(c) PIVOT LOCATION

.0



NASA

Figure 4.- Résumé of propeller whirl trend studies.



NASA

Figure 5.- Flapping-blade propeller whirl model tested in reference 9.

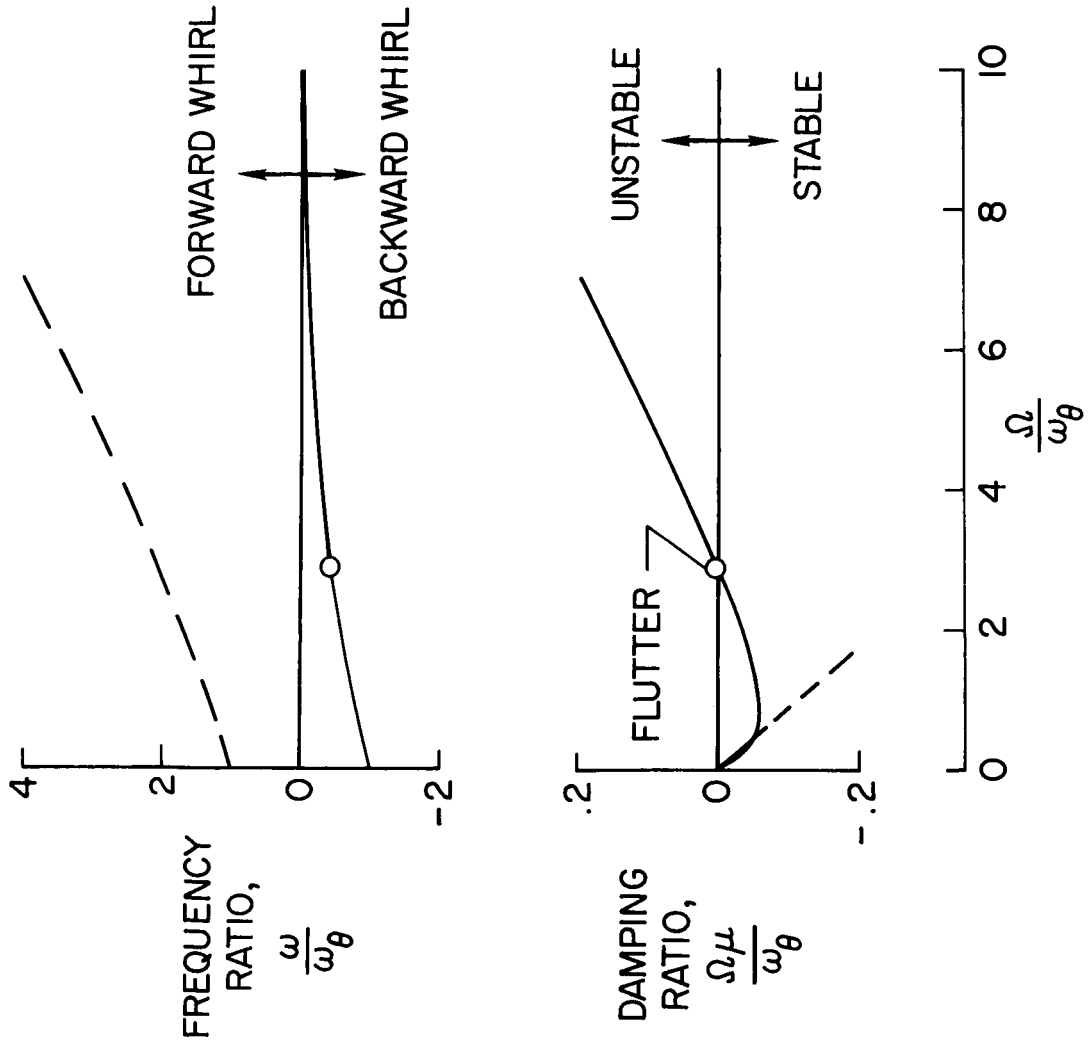


Figure 6.- Calculated rigid-blade whirl modes (see table I).

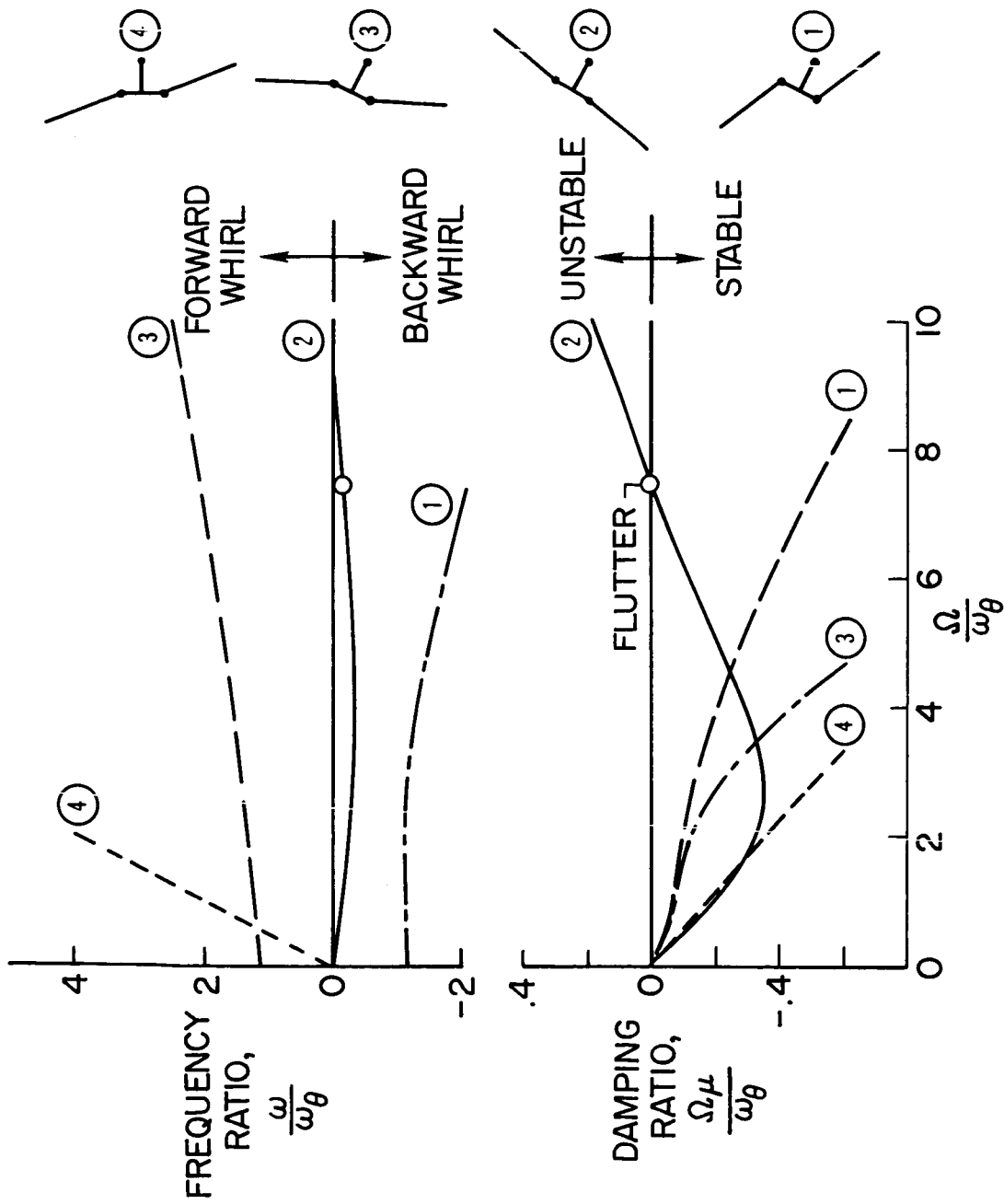


Figure 7.- Calculated flapping-blade whirl modes for  $\frac{e}{R} = 0.13$  (see table I).

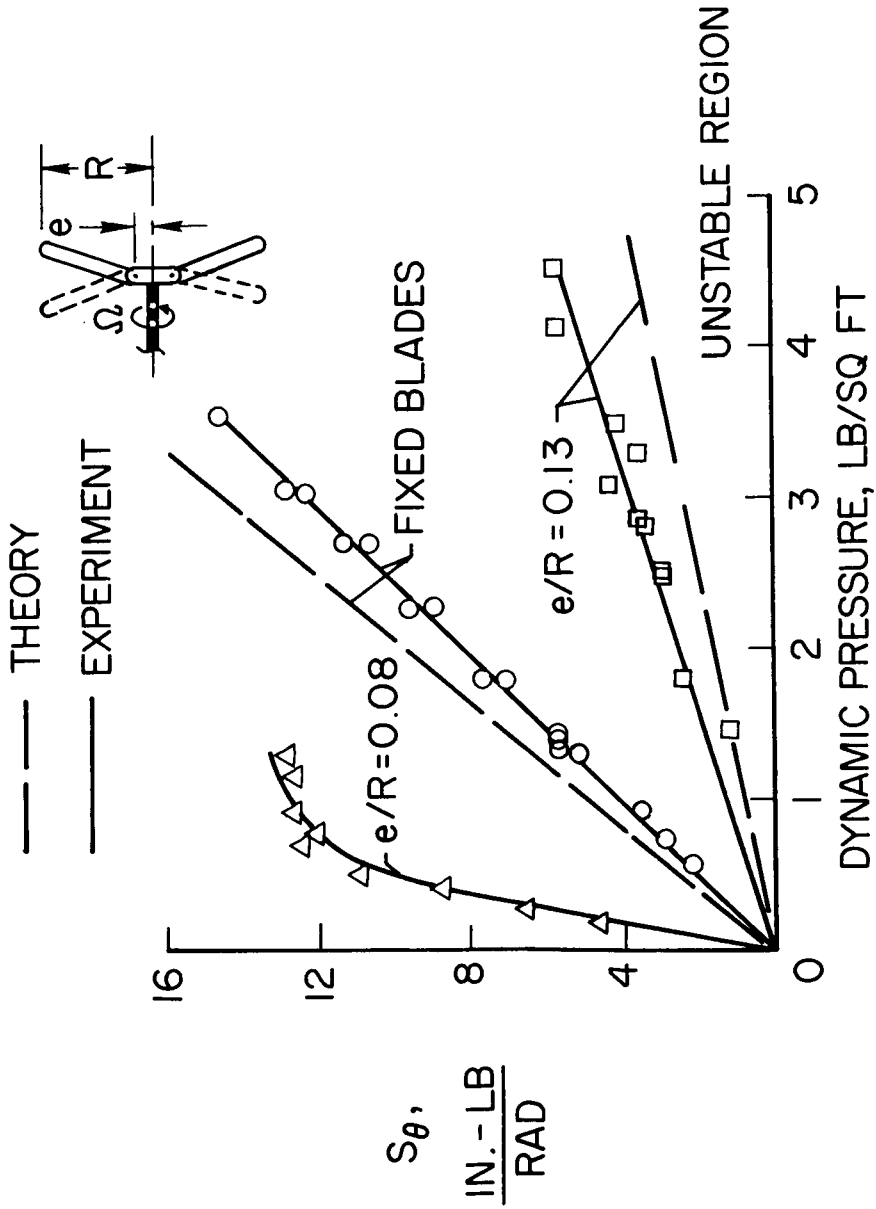
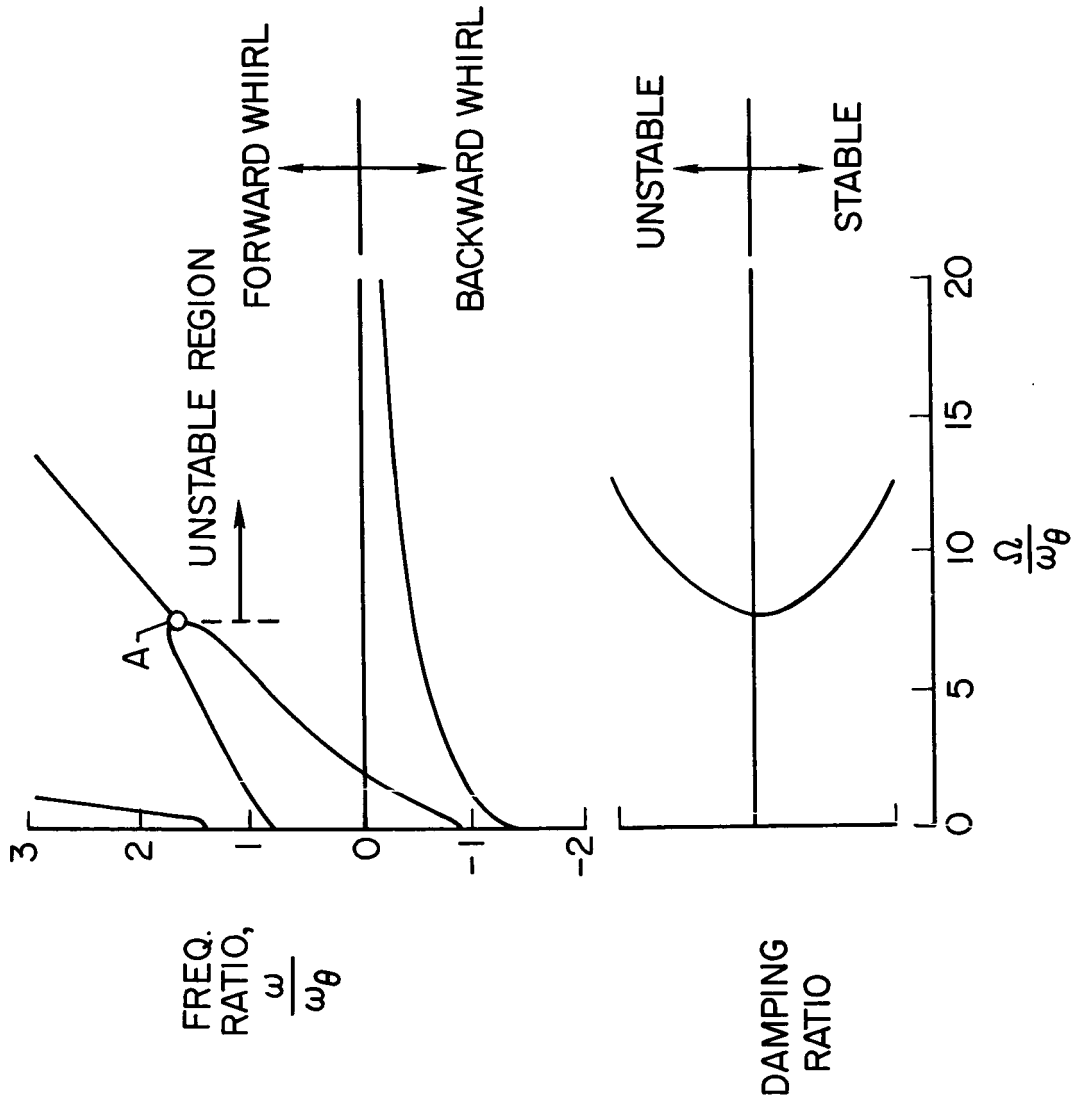


Figure 8.- Comparison of calculated and measured whirl flutter boundaries for flapping-blade model tested in reference 9. (See fig. 5 and table I.)



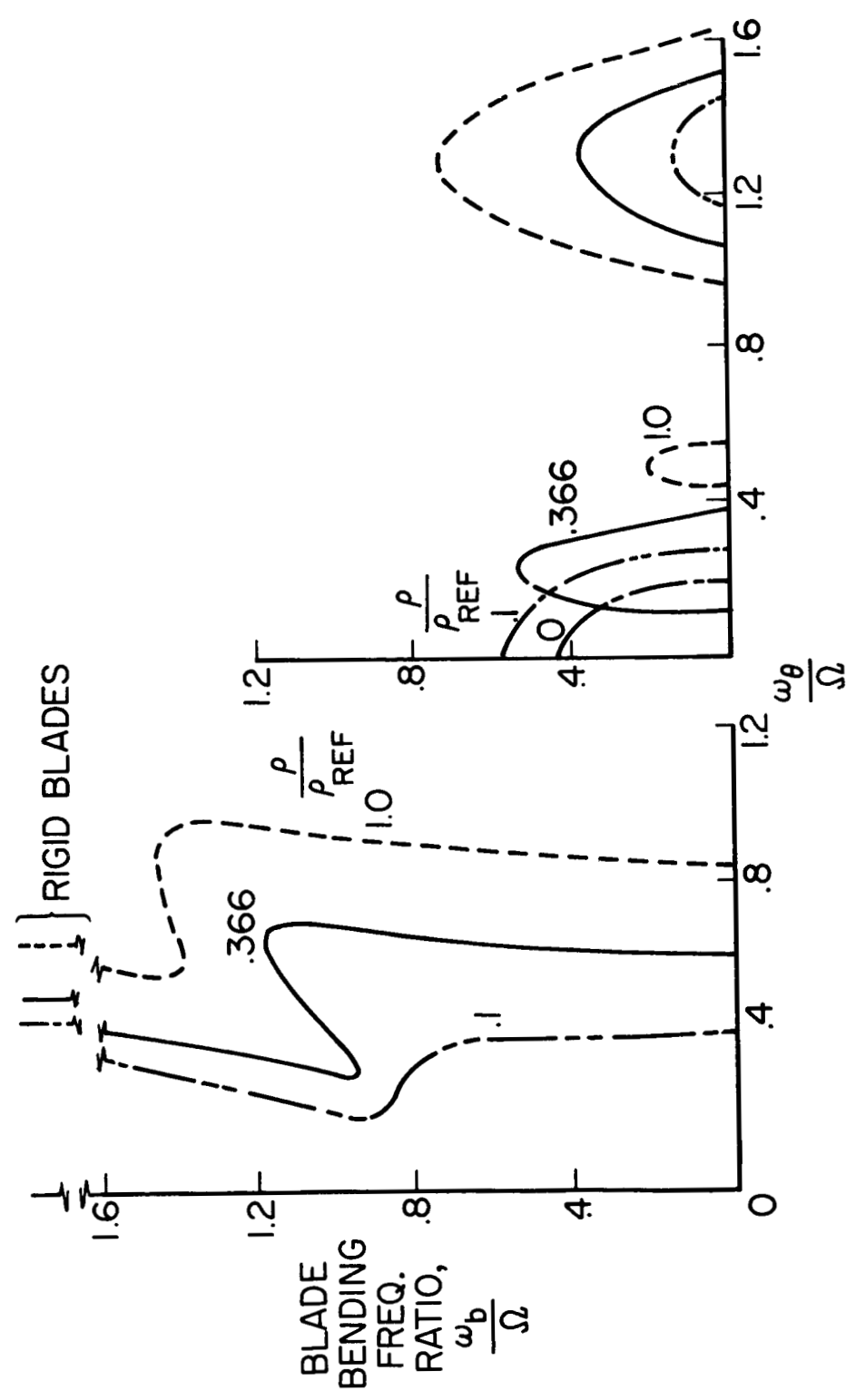
NASA

Figure 9.- Mechanical instability of system with flexible propeller in-vacuo (from ref. 14).



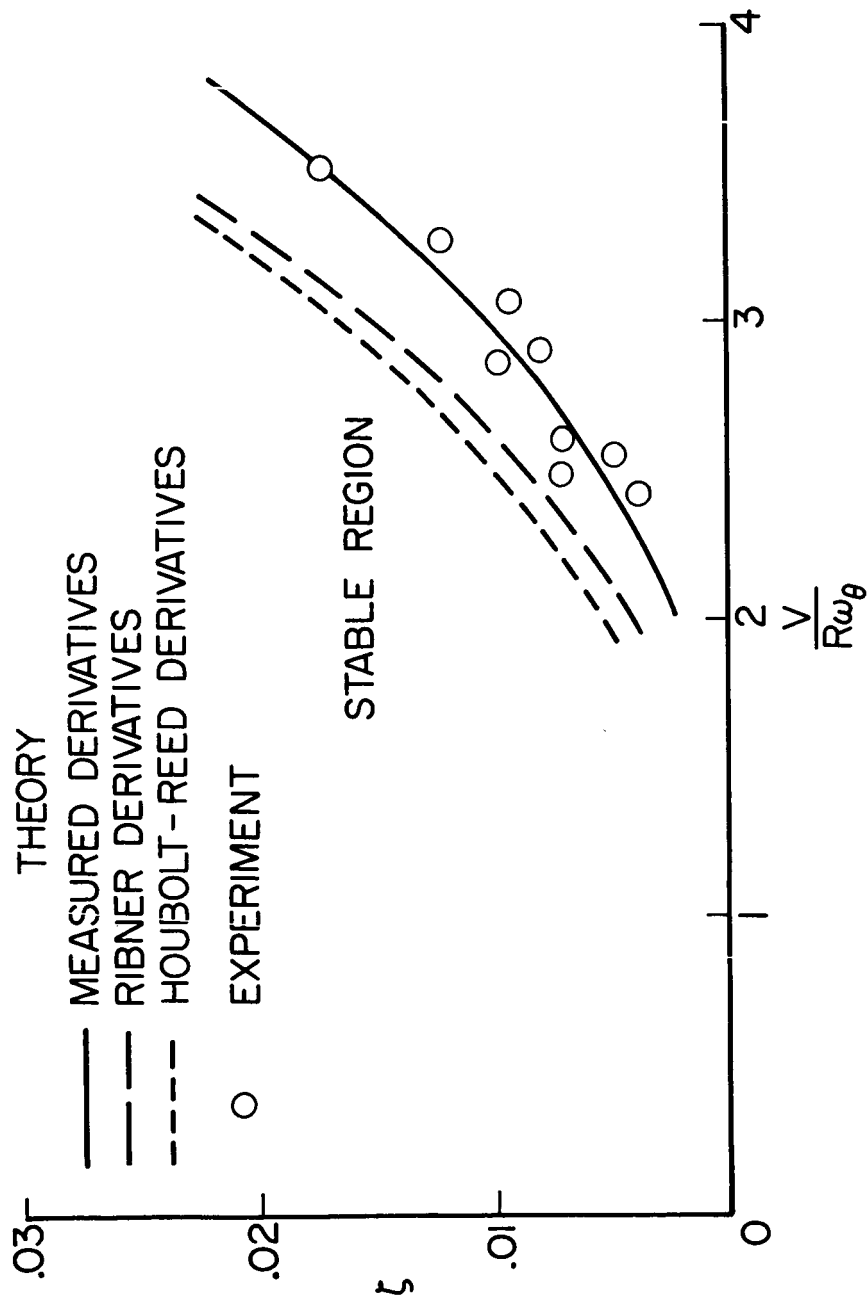
BACKWARD MODE  
("PROPELLER WHIRL")

FORWARD MODE  
("MECHANICAL INSTABILITY")



NASA

Figure 10.- Effect of air density on stability of system with a flexible-blade propeller (from ref. 14).

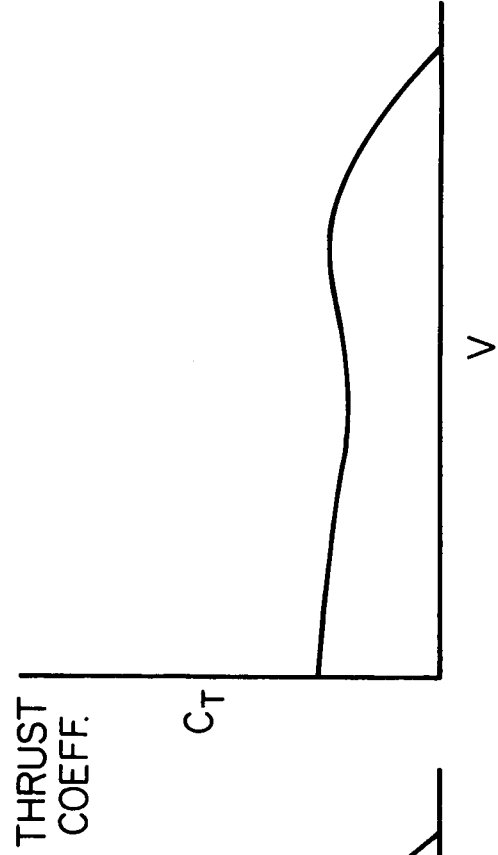
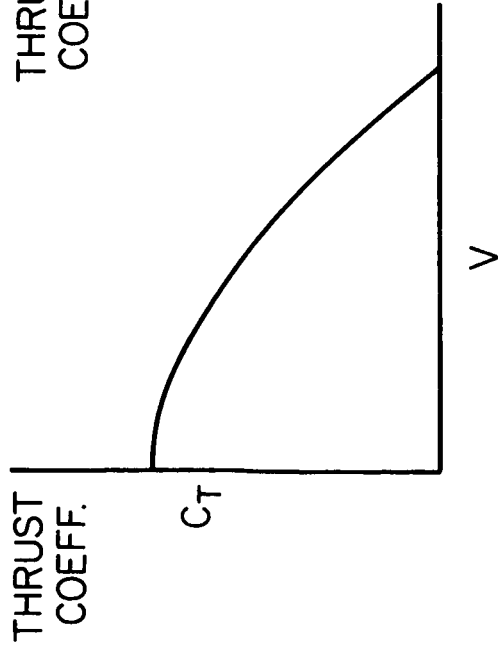


NASA

Figure 11.1.- Comparison of theoretical and experimental whirl flutter boundaries for axisymmetric system with a rigid propeller (from ref. 6).

TYPICAL PROPELLER

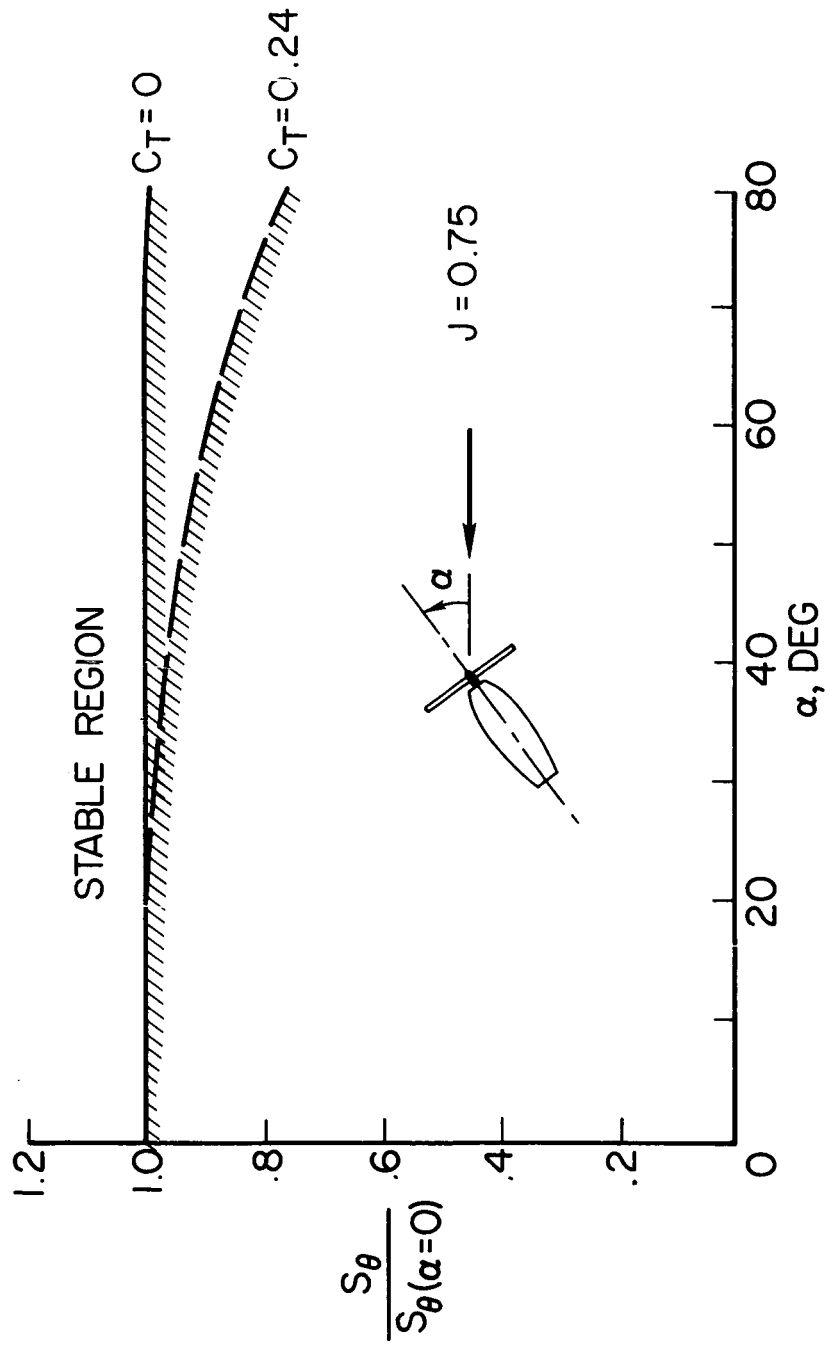
HIGH-SPEED PROPELLER



(a)

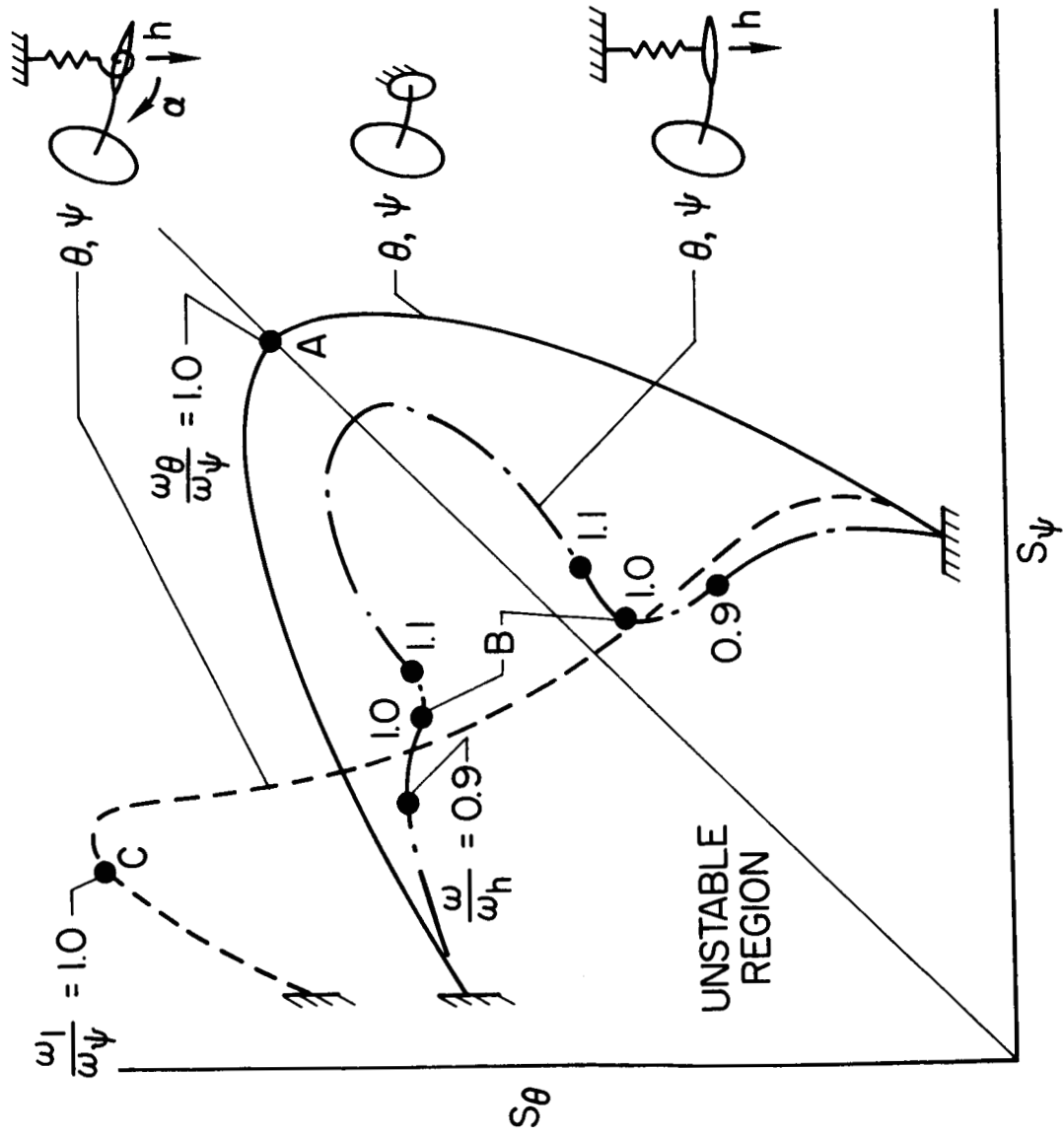
(b)

Figure 12.- Propeller thrust characteristic curves (from ref. 17).



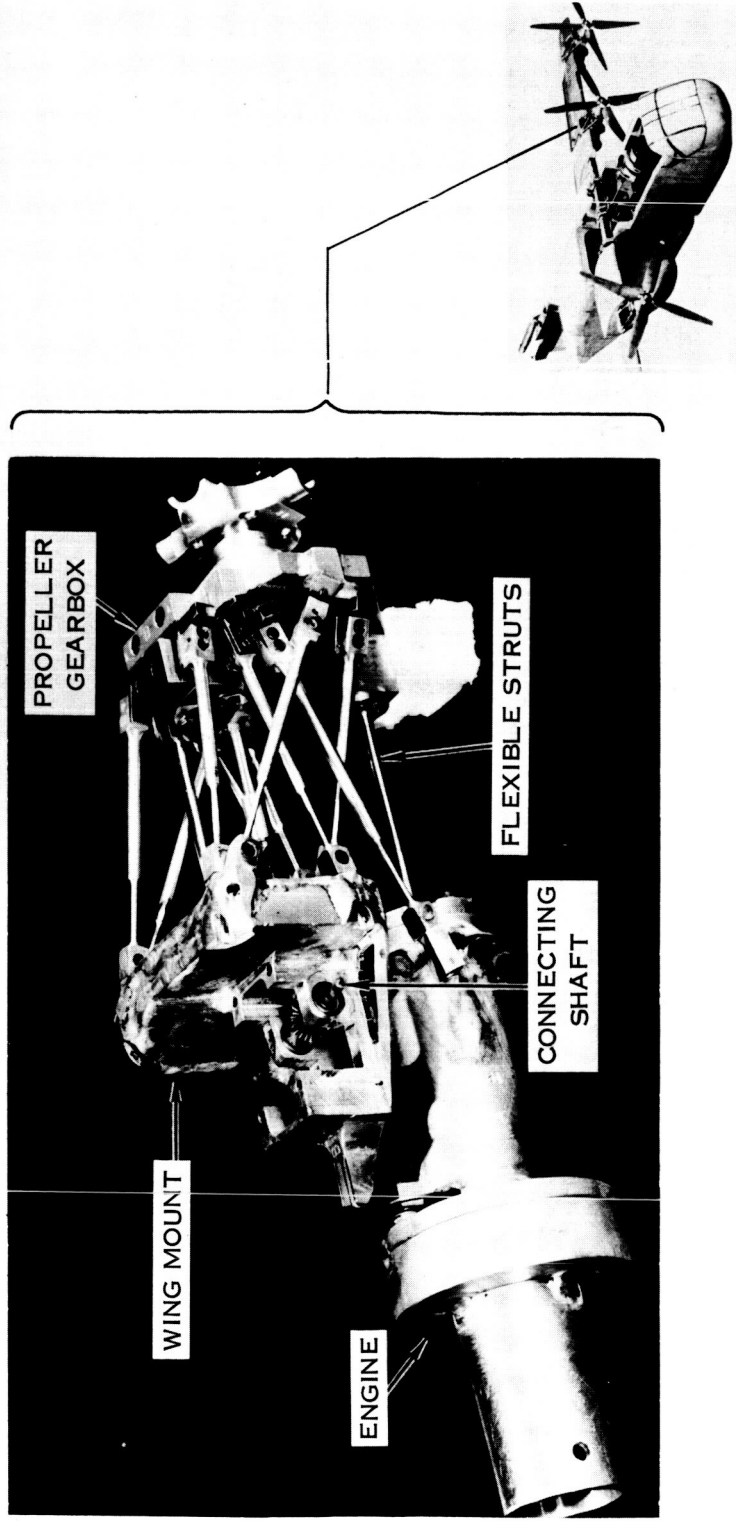
NASA

Figure 13.- Effect of inflow angle on stiffness required to prevent whirl flutter (from ref. 9).



NASA

Figure 14.- Influence of wing flexibility on whirl flutter (adapted from Zwaan and Bergh, ref. 20).



NASA

Figure 15.- Engine-gearbox-propeller system on 1/10-scale dynamically similar model of XC-142A aircraft. (From ref. 22.)